Limnol. Oceanogr., 57(4), 2012, 1084–1098

doi:10.4319/lo.2012.57.4.1084

Increased kinetic efficiency for silicic acid uptake as a driver of summer diatom blooms in the North Pacific subtropical gyre

Jeffrey W. Krause,[a,*] Mark A. Brzezinski,[a,b] Tracy A. Villareal,[c] and Cara Wilson [d]

[a] Marine Science Institute, University of California, Santa Barbara, California
[b] Department of Ecology, Evolution, and Marine Biology, University of California, Santa Barbara, California
[c] Marine Science Institute and the Department of Marine Science, The University of Texas-Austin, Port Aransas, Texas
[d] National Oceanic and Atmospheric Administration and the National Marine Fisheries Service, Southwest Fisheries Science Center, Pacific Grove, California

Abstract

We examined Si limitation of silica production as a factor contributing to summer-bloom dynamics in the North Pacific subtropical gyre (NPSG). Substrate limitation of Si uptake was pervasive, but in most samples the degree of Si limitation was not severe enough to induce growth limitation as observed in the North Atlantic subtropical gyre. These results revise previous interpretations, because the difference in the degree of kinetic limitation between gyres appears to be driven by differences in both substrate and kinetic efficiency. In the NPSG, diatom bloom assemblages tended to show more efficient Si-uptake kinetics and higher Si-uptake rates than did nonbloom assemblages. A bloom dominated by *Mastogloia woodiana* exhibited the most efficient Si-uptake kinetics observed in the ocean to date. Enhanced kinetic efficiency for Si uptake was previously hypothesized to facilitate bloom development, but we suggest the efficient kinetics indirectly affects blooms because $[Si(OH)_4]$ does not appear to limit growth or division rates. Rather, efficient kinetics allows further depletion of the prevailing low $[Si(OH)_4]$ without inducing secondary growth limitation by Si, thereby maximizing biomass yield. Si-uptake limitation was not detected in the lower euphotic zone despite similar $[Si(OH)_4]$ as in well-lit waters, which suggests transition to light limitation of Si uptake with depth. These results suggest that enhanced silica production in the *M. woodiana* bloom was driven by a synergy between diatom species composition, where *M. woodiana* was highly efficient at Si uptake, and high irradiance, which lead to enhanced diatom division rates in the upper euphotic zone.

Phytoplankton blooms in the North Pacific subtropical gyre (NPSG) enigmatically occur during summer under conditions of low nutrients and high water-column stratification (Wilson 2003). Blooms are dominated either by the diazotroph *Trichodesmium* sp. and/or by diatoms of the genera *Hemiaulus, Rhizosolenia,* and *Mastogloia* (Venrick 1974; Villareal et al. 2011); with cells of *Hemiaulus* and *Rhizosolenia* often containing diazotrophs as endosymbionts (Villareal 1991).

Blooms in the NSPG significantly affect regional annual biogeochemical budgets. Summer blooms at the Hawaii Ocean Time-series (HOT) Sta. ALOHA have been estimated to account for 18% of annual new production at that site (Dore et al. 2008). Observations from 150 m and from deep sediment traps at Sta. ALOHA show elevated diatom export associated with summer blooms (Scharek et al. 1999*a*,*b*). Despite the biogeochemical significance of these diatom blooms, a mechanistic understanding of the factors controlling their production is lacking. Here we examine the role of silicic acid limitation in regulating diatom silica production during summer diatom blooms in the NPSG.

Diatoms have an obligate need for silicon during growth, which is used to construct their highly ornate cell wall (frustule). Dissolved orthosilicic acid, $Si(OH)_4$, is the dominant inorganic form (> 95%) of silicon available at seawater pH, and diatoms actively transport $Si(OH)_4$ immediately prior to silica polymerization and cell division (Brzezinski et al. 1990). The response of the specific rate of Si uptake (V_b) to increasing $[Si(OH)_4]$ conforms to a rectangular hyperbola described by the Michaelis–Menten function (Nelson et al. 1976; Nelson and Dortch 1996):

$$V_b = \frac{V_{max}[Si(OH)_4]}{K_S + [Si(OH)_4]} \quad (1)$$

where V_{max} is the maximum specific uptake rate (the hyperbola asymptote) and K_S is the half-saturation concentration (i.e., the $[Si(OH)_4]$ where $V_b = ½\ V_{max}$ [note V_b at the ambient $[Si(OH)_4]$ will be denoted as V_{amb}]). In both the North Atlantic subtropical gyre (NASG) and in the NPSG, previous studies have shown that low ambient $[Si(OH)_4]$ restrict Si-uptake rates to 10–50% of V_{max} (Brzezinski and Nelson 1996; Brzezinski et al. 1998). The exception occurred during a summer bloom in the NPSG where the diatoms were taking up Si at ~ 70% of their potential maximum rate (Brzezinski et al. 1998). That observation led Brzezinski et al. (1998) to propose that high kinetic efficiency facilitated the development of these blooms without a change in silicic acid supply. Whether high kinetic efficiency is a common feature of summer diatom blooms in the NPSG is unknown. Here, we report results from field experiments examining Si-uptake kinetics in the NPSG to test the hypothesis that highly efficient Si-uptake kinetics are characteristic of summer diatom blooms in the NPSG and to explore potential factors controlling kinetic efficiency of bloom diatom assemblages.

* Corresponding author: jeffrey.krause@lifesci.ucsb.edu

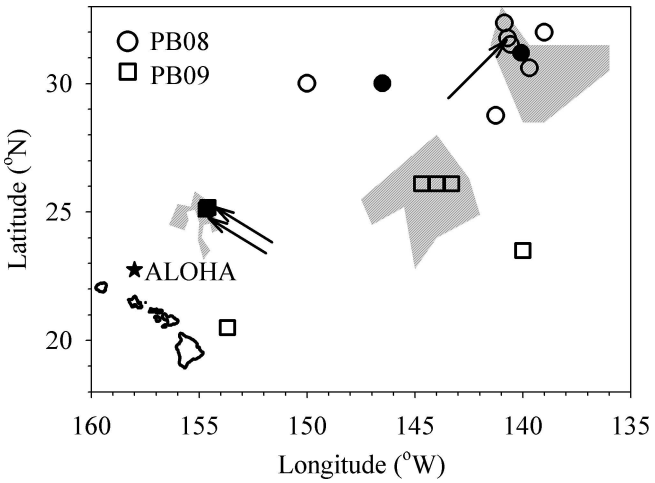

Fig. 1. Kinetic experiment station locations during the PB08 and PB09 cruises; Sta. ALOHA is shown for reference (star). Symbols are distinguished by kinetic experiment type: eight-point (open symbols) and two-point (closed symbols); arrows point to the bloom stations. Outlines show the maximum spatial extent of each transient bloom by a time-integrated depiction of the area where surface Chl was > 120 ng L^{-1} (MODIS ocean color data).

Methods

The Pacific open-ocean Bloom (PB) cruises were carried out aboard the R/V *Kilo Moana* from 4 to 19 July 2008 (PB08) and 29 July to 12 August 2009 (PB09). Daily-composite images from the Moderate Resolution Imaging Spectroradiometer (MODIS, http://modis.gsfc.nasa.gov) were used to locate blooms defined as surface chlorophyll a (Chl *a*) concentrations of ≥ 120 ng L^{-1}. Specific diatom-bloom stations were identified by fulfillment of two data-based criteria: (1) the > 10 μm size-fraction [Chl *a*] was $>$ 30% of the total (> 0.4 μm) [Chl *a*], this value is three-fold higher than the $< 10\%$ contribution of > 10-μm cells to total [Chl *a*] under background conditions in the eastern gyre during summer (Villareal et al. 2011); and (2) diatom numerical abundances were > 1000 cells L^{-1}, consistent with bloom abundances previously observed in this region (Brzezinski et al. 1998; Villareal et al. 2011). PB08 sampling focused on a region to the northeast of Hawaii near the subtropical front (Fig. 1) where one bloom station was sampled (Sta. 7; Table 1). During PB09, a high [Chl *a*] feature developed east of Hawaii but faded by the time of sampling (Fig. 1); however, another bloom developed to the north of Hawaii during the cruise and two stations were sampled in that feature while it was still well-developed (Fig. 1).

Experiments examining the kinetics of silicic acid use were conducted to assess the response of the ambient diatom community to increased $Si(OH)_4$ availability. These experiments were performed at each station using water from the depth where 59% of the irradiance was available (range = 8–18 m; Table 1), measured using a photosynthetically available radiation (PAR) sensor, relative to the irradiance at a reference depth just below the sea surface (100% I_0). Most experiments examined the response of Si uptake to eight silicic acid concentrations between ambient and + 20 μmol L^{-1} (open symbols, Fig. 1). Additional experiments were performed to assess whether Si-uptake kinetics varied with depth. Samples were taken at the additional light depths of 100%, 31%, 19%, 10%, 6%, and 3.4% I_0 and two-point kinetic experiments were conducted by measuring uptake at only two substrate concentrations: ambient and + 20 μmol L^{-1} $[Si(OH)_4]$ (filled symbols, Fig. 1).

Seawater for all kinetic experiments was collected using 12-liter sampling bottles on a rosette equipped with a Seabird profiler and PAR sensor. Casts were taken between 04:00 h and 06:00 h (local time). The volume of seawater required for each experiment was drained from the sampling bottles into a single polycarbonate container and mixed just prior to being subsampled for Si-uptake rate measurements, the measurement of $Si(OH)_4$ concentration and diatom biomass as biogenic silica ($bSiO_2$) concentration. Separate samples for phytoplankton taxonomic composition and size-fractionated Chl *a* also were taken from the same Niskin bottle as was used for the kinetic experiments.

Unfiltered samples for $[Si(OH)_4]$ analysis were dispensed into 50-mL polypropylene tubes and refrigerated at 4°C until analysis (< 4 h) at sea using a sensitive manual colorimetric method (Brzezinski and Nelson 1995). Seawater for $bSiO_2$ analysis was collected in 2.8-liter polycarbonate bottles, filtered through 0.6-μm polycarbonate filters, and analyzed using a NaOH digestion procedure (Brzezinski and Nelson 1995) in Teflon tubes, which provide low and stable blanks (Krause et al. 2009). Diatom abundance was enumerated using the Utermöhl method (Utermöhl 1958). Total abundance was determined to be the sum of four dominant diatom groups (*Hemiaulus hauckii, Rhizosolenia* spp., *Mastogloia woodiana,* and *Chaetoceros* spp.); these four groups have been previously observed to comprise nearly all the diatom community during summer blooms (Venrick 1974; Brzezinski et al. 1998; Villareal et al. 2011) and all but *M. woodiana* can harbor diazotroph symbionts (Foster and Zehr 2006). Both *Rhizosolenia* spp. and *Chaetoceros* spp. include taxa that were not associated with diazotrophic symbionts. Due to *M. woodiana*'s small size, its identity was confirmed from Sta. 23 (PB09) samples by using scanning electron microscopy. Small pennates of similar morphology and size observed in Utermöhl chambers were categorized as *M. woodiana,* although it is likely that other small pennate diatoms were included in this category (Villareal et al. 2012). [Chl *a*] was determined for the > 0.4 μm (e.g., total phytoplankton community) and > 10 μm (e.g., diatoms, dinoflagellates) size-fractions by filtering 250 mL and 500 mL, respectively, through polycarbonate membrane filters, extracting in methanol, and quantifying fluorometrically without acidification (Welschmeyer 1994).

All Si-uptake experiments were conducted in polycarbonate bottles (300 mL) using high specific activity ^{32}Si, > 40 kBq (μmol Si)$^{-1}$, as aqueous $NaSiO_2$. Seawater was dispensed into seven incubation bottles, and then nonradioactive aqueous sodium metasilicate was added to enhance the $[Si(OH)_4]$ by 1.5, 2.5, 3.0, 4.0, 7.5, 12.0, 20.0 μmol L^{-1}, with an eighth bottle receiving no

Table 1. Physical, chemical, and biological setting for PB cruise stations at 59%I_0 and Sta. ALOHA during July–August (data courtesy of the HOT program) and all other months, ± SE. PB nutrients and ALOHA data are averages of all data available in the upper 30 m ([NO_3] data from PB08 cruise courtesy of M. Church, [SRP] data from Duhamel et al. 2010, 2011). The numerically dominate diatom is reported (*see* Methods for main diatom groups), and the value within the parentheses indicates the percentage of the total diatom abundance from the dominate diatom. Below detection denoted as 'bd' (note—only autoanalyzer samples were taken for [NO_3] during PB09).

Cruise	Station	Local date	Lat. (°N)	Long. (°W)	Depth of 59% I_0 (m)	Temp (°C)	MLD (m)	[NO_3] (μmol L^{-1})	[SRP] (μmol L^{-1})	Chl *a* >0.4μm (ng L^{-1})	Chl *a* >10μm (ng L^{-1})	Diatoms (cells L^{-1})	Dominant diatom (%)
PB08	1	04 Jul	30.00	150.00	8	22.9	7	0.003	0.034	50	7	220	*H. hauckii* (63.6)
	2*	05 Jul	30.00	146.50	15	22.8	27	0.002	0.033	56	10	331	*H. hauckii* (48.3)
	3	07 Jul	32.35	140.86	15	21.4	11	0.005	0.049	137	7	139	*H. hauckii* (66.9)
	7†	09 Jul	31.77	140.71	12	21.8	11	0.003	0.052	95	39	1648	*H. hauckii* (84.1)
	9*	10 Jul	31.19	140.08	18	19.1	31	—	—	81	8	191	*H. hauckii* (84.8)
	12	12 Jul	30.61	139.70	10	21.7	25	0.007	0.080	62	12	123	*H. hauckii* (72.4)
	14	13 Jul	28.75	141.25	13	22.4	24	0.007	0.033	67	10	204	*H. hauckii* (72.5)
	15	14 Jul	31.52	140.58	11	22.1	26	0.005	0.055	78	13	—	—
	16	15 Jul	32.00	139.00	11	21.7	25	0.005	0.074	71	10	6	*H. hauckii* (83.3)
Bloom						21.8	11	0.003	0.052	95	39	1648	*H. hauckii*
Nonbloom mean ± SE						21.8±0.4	22±3	0.005±0.001	0.051±0.008	75±10	10±1	138±38	*H. hauckii*
PB09	1	30 Jul	20.50	153.69	14	25.8	10	bd	0.121	65	11	100	*H. hauckii* (99.0)
	3	02 Aug	26.10	144.70	13	23.6	41	bd	0.031	50	5	40	*M. woodiana* (80.0)
	7	03 Aug	26.10	144.00	12	23.7	54	bd	0.017	13	1	0	—
	11	04 Aug	26.10	143.30	16	23.1	47	bd	0.090	43	3	20	*M. woodiana* (55.0)
	21	09 Aug	23.50	140.00	12	23.5	46	bd	0.153	57	4	4	*M. woodiana* (100.0)
	22*,†	12 Aug	25.10	154.70	11	25.8	48	bd	0.027	391	193	5183	*M. woodiana* (98.7)
	23†	12 Aug	25.18	154.60	11	25.7	50	bd	—	226	225	16610	*M. woodiana* (96.3)
Bloom mean ± SE						25.8±<0.1	49±1	—	0.027	308±83	209±16	10,897±5713	*M. woodiana*
Nonbloom mean ± SE						23.9±0.5	40±8	—	0.082±0.026	46±9	5±2	37±18	*M. woodiana*
Sta. ALOHA Jul–Aug (1999–2009) mean ± SE					<30	26.0±<0.1	48±2	0.003±<0.001	0.056±0.005	93±3	—	—	—
Sta. ALOHA Sep–Jun (1999–2009) mean ± SE					<30	24.7±<0.1	66±3	0.003±<0.001	0.048±0.002	104±2	—	—	—

* Two-point kinetic experiments only.
† Bloom station.

additional Si. $^{32}Si(OH)_4$ tracer was cleaned of trace metals by passage through Chelex resin prior to experimental use. Isotope additions were 360 Bq for experiments during PB08, but during PB09 this was increased to 1085 Bq for samples amended with > 7.5 μmol L^{-1} to increase measurement sensitivity by enhancing the final specific activity of the tracer. The addition of the tracer increased ambient $[Si(OH)_4]$ by < 0.001 μmol L^{-1}. ^{32}Si blanks were made by adding 360 Bq of ^{32}Si to 0.2-μm-filtered seawater and immediately processing (below). After tracer addition, bottle contents were mixed and the samples incubated in acrylic deck incubators screened with neutral density screens to match the light level at the depth of collection. Samples were incubated for 12 h while they were continuously cooled by a flow of surface seawater.

After incubation, all samples were filtered using 0.6-μm pore size, 25-mm-diameter polycarbonate filters under gentle vacuum (< 33 kPa), and then rinsed with 0.2-μm-filtered seawater to remove excess tracer not incorporated within particles. Filters were dried on nylon planchettes, covered with Mylar film, and processed for measurement of ^{32}Si activity using gas-flow proportional counting at secular equilibrium (Krause et al. 2011). Gross silica production rates were calculated (nmol Si L^{-1} h^{-1}) and normalized by $[bSiO_2]$ (nmol Si L^{-1}) to derive specific Si-uptake rates (V_b, h^{-1}), as in Brzezinski and Phillips (1997).

Data from the kinetic experiments were quality-controlled and processed using established protocols. Samples with ^{32}Si activities below the detection limit, defined as 2σ of the ^{32}Si filter blanks (Blank $\pm$ 2σ = 0.05 $\pm$ 0.03 Bq), were discarded. This occurred occasionally for the high Si additions due to the decrease in specific activity at high Si additions, which decreased the sensitivity of the measurement. For the eight-point experiments, statistical outliers were identified by applying a linear Woolf transformation of the Michaelis–Menten function and fitting a least-squares regression (Brzezinski et al. 2008). If the residual for any point was $> 2\sigma$ of all residuals in an experiment, it was considered an outlier and removed. This resulted in the removal of no more than one point from any given experiment. After removal of outliers, V_{max} and K_S were calculated using a nonlinear curve-fitting algorithm in SigmaPlot 10.0©.

The rates obtained from the two-point kinetic experiments were used to examine uptake kinetics in two ways. The first assumes that the + 20 μmol L^{-1} addition saturates Si uptake given the observed low $[Si(OH)_4]$ in the NPSG. Thus, the ratio of the rate at the ambient silicic acid concentration, V_{amb}, to the rate at the + 20 μmol L^{-1} addition of $Si(OH)_4$ approximates $V_{amb}:V_{max}$. A ratio of $V_{amb}:V_{max} < 1.0$ indicates the ambient $[Si(OH)_4]$ does not support the maximum Si uptake; because of analytical uncertainties in rate measurements $V_{amb}:V_{max}$ must be < 0.92. This is better than the 0.83 value reported by Nelson et al. (2001), with the improvement due to increased precision in both the $[bSiO_2]$ and ^{32}Si measurements. The second analysis assumes that the rates at ambient and + 20 μmol L^{-1} $[Si(OH)_4]$ represent two points falling exactly on a Michaelis–Menten hyperbola, allowing estimates of both V_{max} and K_S to be computed as described by Nelson et al. (2001).

Other data sets from the PB cruises and from Sta. ALOHA are reported for environmental context. Concentrations of nitrate $[NO_3]$ during both cruises were determined on shore using a LaChat Quikchem 8000 analyzer for unfiltered samples, which were immediately frozen and thawed prior to analysis; however, during PB08 $[NO_3]$ was also measured by using the more sensitive chemoluminescence method (data courtesy of M. Church) used by the HOT program (Church et al. 2009). Soluble reactive phosphorus [SRP] was determined using a high-sensitivity brucite precipitation method (SRP data and method from Duhamel et al. 2010, 2011). For comparison, data from Sta. ALOHA by the HOT program (e.g., hydrography, NO_3, SRP, Chl *a*) are reported along with kinetic experiment results (e.g., Si uptake, $Si(OH)_4$, $bSiO_2$) from a 2-yr study of silicon biogeochemistry at Sta. ALOHA (Brzezinski et al. 2011) where, from January 2008 through December 2009, two-point kinetic experiments similar in design to those reported here (i.e., ambient and + 20 μmol L^{-1} $Si(OH)_4$) were conducted during HOT cruises using water collected from 25-m depth. We used the rates obtained by Brzezinski et al. (2011) to calculate V_{max} and K_S by using the Nelson et al. (2001) approach for all experiment where significant Si limitation was detected (e.g., $V_{amb}:V_{max} < 0.92$).

Results

Measurements at 3 of the 16 stations sampled, 1 during PB08 and 2 during PB09, met the diatom bloom criteria (Table 1; Fig. 1), with the PB08 bloom being in a state of decline when sampled. Our criteria for a diatom bloom at specific stations is not applicable to the entire phytoplankton community (i.e., when all phytoplankton groups increase biomass). Dore et al. (2008) defined 8.7 mg Chl *a* m^{-2} as the minimum 0–80-m integrated [Chl *a*] for summer blooms a Sta. ALOHA. During the PB08 bloom, the 0–80-m integrated [Chl *a*] was 8.2 mg Chl *a* m^{-2}, while the PB09 bloom stations ranged from 31 mg Chl *a* m^{-2} to 35 mg Chl *a* m^{-2} (Villareal et al. 2012). The lower integrated [Chl *a*] in the PB08 bloom is consistent with it being in a state of decline, while the PB09 bloom at the time of sampling was well-developed and, as will be described below, very active.

Physical conditions and standing stock measurements—The physical and chemical environment during the PB cruises is briefly described for context. The waters sampled near the subtropical front during PB08 were cooler compared with average temperatures during this time of year at Sta. ALOHA closer to Hawaii (Table 1), whereas many PB09 stations were of a similar temperature to Sta. ALOHA (Table 1). Salinity differences were observed between cruises (data not shown) and were due to sampling near the subtropical front during PB08, which is characterized by lower and more variable salinity than observed in the gyre interior (Shcherbina et al. 2009, 2010). The mixed-layer depth (MLD), defined by a 0.125-kg m^{-3} potential density change from the surface was shallow during PB08 (range = 7–31m). At the bloom station, MLD was 11 m vs.

22 ± 3 m (error is SD unless otherwise stated) at the nonbloom stations. However, during PB09, the trend of shallower MLD at the bloom stations reversed. MLD at the bloom stations was 49 ± 1 m, vs. 40 ± 7 m at nonbloom stations. Blooms during both years occurred when MLD depths were < 50 m, consistent with previous observations that the MLD for summer blooms near Sta. ALOHA (i.e., gyre interior) is generally < 45 ± 15 m (White et al. 2007).

Consistent with gyre conditions, the concentrations of inorganic nutrients were very low. Dissolved silicate at the 59%I_0 (Tables 2, 3) was consistently one or two orders of magnitude higher than either [NO_3] or [SRP] (Table 1). The PB08 average [$Si(OH)_4$] at nonbloom stations was ~ 0.5 μmol L^{-1} higher than at the bloom station (1.26 μmol L^{-1}; Table 2). This was similar during PB09, but the bloom average [$Si(OH)_4$] was even lower (0.85 μmol L^{-1}; Table 2) than during the PB08 bloom and was also lower than nearly all observations at Sta. ALOHA during 2008 and 2009 (Brzezinski et al. 2011). Nonbloom stations during PB09 had lower [$Si(OH)_4$] (1.14 μmol L^{-1}) than both bloom and nonbloom stations during PB08 (Table 2). This is consistent with the satellite observation that many of the nonbloom stations during PB09 were sampled after the decline of high-chlorophyll conditions. The tendency for the observation of lower [$Si(OH)_4$] at the bloom stations during both cruises implies depletion within blooms.

Within blooms, the increase in diatom cell abundance was accompanied by a shift to a higher proportion of total [Chl *a*] in the > 10-μm size fraction. *H. hauckii* and *M. woodiana* numerically dominated the PB08 and PB09 blooms, respectively, and diatom abundance in both blooms was at least an order of magnitude higher than those at nonbloom stations (Table 1). All enumerated diatom genera attained high abundance within blooms, but the rank order of abundance among blooms differed (Villareal et al. 2012). During the PB08 bloom, the > 10-μm [Chl *a*] was nearly four-fold higher than at nonbloom stations, and the disparity was even higher between bloom and nonbloom stations during PB09 (Table 1). The proportion of total [Chl *a*] (> 0.4 μm) in the > 10-μm size fraction ranged between 10% and 14% at the nonbloom stations during both cruises. This proportion increased to 41% and ~ 49–100% in the PB08 and PB09 blooms, respectively. Biogenic silica concentrations generally mirrored the > 10-μm [Chl *a*]. [$bSiO_2$] during the PB08 bloom was 197.5 nmol Si L^{-1}, whereas the mean for nonbloom stations was 38.4 nmol Si L^{-1} (Table 2). During PB09, there was a similar difference between bloom and nonbloom station [$bSiO_2$], with bloom values of 92.9 nmol Si L^{-1} (Table 2) and 64.1 nmol Si L^{-1} (59%I_0, Table 3) but a mean of 15.7 nmol Si L^{-1} for nonbloom stations (Table 2). The high [$bSiO_2$] at bloom stations coincided with the observed draw-down in [$Si(OH)_4$] and high diatom abundance.

Kinetics of Si use—The eight-point kinetic experiments generally showed saturation of Si uptake at high [$Si(OH)_4$] following Michaelis–Menten kinetics (Fig. 2). One experiment exhibited a near-linear response (Fig. 2A), as seen occasionally by Brzezinski et al. (1998) in the NPSG and in the NASG by Brzezinski and Nelson (1996). This linearity in uptake at Sta. 1 (PB08) made for both high and less-constrained estimates of V_{max} and K_S (Table 2). Because of the disparity (i.e., linear uptake) with other stations, kinetic data from this station were omitted for calculation of mean kinetic-parameters values from nonbloom stations.

Calculation of kinetic parameters from two-point experiments requires the assumption that the uptake rates at the two concentrations fall exactly on a Michaelis–Menten rectangular hyperbola. To test this assumption, the kinetic parameters from each eight-point kinetic experiment were compared with kinetic parameters calculated using just the rate information at the ambient and + 20 μmol L^{-1} [$Si(OH)_4$] from the same experiments. The experiment showing linear kinetics and specific experiments where the V_b at + 20 μmol L^{-1} was below detection were omitted from the comparative analysis. Also, if V_b at + 20 μmol L^{-1} was ≤ V_{amb}, K_S could not be successfully calculated using a two-point approach. Model-II linear regression was used to compare parameter estimates using the two approaches (Fig. 3). The V_{max} obtained from the two-point algebraic calculation was 95% ± 8% (± SE, r^2 = 0.93, p = 0.002) of the V_{max} calculated by eight-point nonlinear regression (Fig. 3A); however, the relationship could be highly influenced by the one high rate (Fig. 3). To test for a possible bias driven by the one very high value of observed trend for V_{max}, the analysis was repeated without those data, with the result that V_{max} from the two-point estimation was 103% ± 25% (± SE, r^2 = 0.45, p = 0.016) of the eight-point calculation, although the strength of the model-II linear regression is less (r^2 lowered). The lower calculated V_{max} from the two-point experiments is consistent with V_b in the + 20 μmol L^{-1} [$Si(OH)_4$] falling below the nonlinear curve fit in multiple experiments (e.g., Fig. 2B–D). These results suggest that V_{max} calculated using a two-point experiment will likely fall between 76% and 113% (95% CI of the slope) of the eight-point experiment V_{max}. The values of K_S estimated from two vs. eight silicic acid concentrations averaged 103% of the value calculated by nonlinear regression (Fig. 3B), with a 95% CI of between 80% and 126%. To assess relative error associated with the derived ratios, $V_{amb}:V_{max}$ and $V_{max}:K_S$, values calculated using both the eight-point and two-point approaches were compared. The standard deviation of the difference between the estimates gave a relative uncertainty of ± 16% and ± 44% of the average values for $V_{max}:K_S$ and $V_{amb}:V_{max}$, respectively.

Ambient and maximum uptake rates increased proportionally. V_{amb} and V_{max} from the eight-point experiments were positively and significantly correlated (Model-II linear regression, slope ± SE 1.56 ± 0.12, r^2 = 0.95, p < 0.001); however, this may be an artifact because the nonlinear-regression calculation of V_{max} is partially influenced by V_{amb} and hence not independent. To test the robustness of this finding, we also examined the relationship when only using V_{amb} and V_b at + 20 μmol L^{-1}—which does not force V_{max} to conform to the Michaelis–Menten function. This approach also showed a strong correlation between V_{amb} and V_{max} (Model-II linear regression, slope ± SE 1.47 ± 0.12, r^2 = 0.93, p = 0.001),

Table 2. Station by station results from eight-point kinetic experiments at 59%I_0, error term is ± SE. Also shown are the concentrations of dissolved silicate [$Si(OH)_4$] and biogenic silica [$bSiO_2$]. For comparison, data from Sta. ALOHA are shown for summer ($n = 4$) and nonsummer months ($n = 14$; Brzezinski et al. 2011). Because of the linear kinetics, parameters using V_{max} and K_S from PB08 Sta. 1 were not used for the PB08 nonbloom means. [$Si(OH)_4$], [$bSiO_2$], and V_{amb} data from PB08 Sta. 2 and 9, and PB09 Sta. 22 at 59%I_0 (two-point kinetic experiment stations, *see* Table 3), are included in either the nonbloom or bloom means. Error terms for V_{amb} : V_{max}, V_{max} : K_S, and kinetic-parameter means (where applicable) are derived using error propagation.

Cruise	Station	[$Si(OH)_4$] (μmol L^{-1})	[$bSiO_2$] (nmol Si L^{-1})	V_{amb} (h^{-1})	V_{max} (h^{-1})	K_s (μmol L^{-1})	V_{amb} : V_{max} (%)	V_{max} : K_s (mmol L^{-1} $h)^{-1}$
PB08	1	2.13	22.4	0.009	0.306±0.264	75.00±76.32	2.8±3.4	4.1±5.4
	3	1.75	58.4	0.002	0.004±0.001	2.09±1.22	45.5±11.2	2.1±1.3
	7*	1.26	197.5	0.005	0.009±0.001	0.83±0.30	60.5±5.4	11.3±4.2
	12	1.57	44.0	0.002	0.004±<0.001	0.81±0.41	65.8±10.8	4.3±2.2
	14	1.50	21.4	0.006	0.009±0.002	0.59±0.79	71.7±19.3	14.9±20.1
	15	1.64	61.9	0.004	0.008±0.001	1.60±0.75	50.7±8.8	5.3±2.6
	16	2.05	25.3	0.003	0.006±0.002	1.57±1.59	56.6±24.0	3.8±4.0
Bloom		1.26	197.5	0.005	0.009±0.001	0.83±0.30	60.5±5.4	11.3±4.2
Nonbloom mean ± SE		1.72±0.08	38.4±5.6	0.004±0.001	0.006±0.001	1.33±0.58	58.1±8.9	6.1±5.2
PB09	1	1.19	18.0	0.004	0.007±0.001	0.98±0.69	54.9±10.7	7.4±5.3
	3	0.98	17.2	0.002	0.006±0.002	2.12±2.43	31.7±17.4	2.8±3.4
	7	0.87	15.0	0.002	0.004±0.001	0.92±0.88	48.6±14.6	4.8±4.7
	11	1.34	16.0	0.002	0.008±0.005	2.01±4.08	40.0±33.3	3.8±8.1
	21	1.29	12.4	0.003	0.005±0.001	0.72±1.18	64.1±27.0	6.3±10.3
	23*	0.82	92.9	0.015	0.025±0.002	0.34±0.24	70.4±8.1	72.9±52.1
Bloom mean ± SE		0.85±0.03	78.5±14.4	0.017±0.002	0.025±0.002	0.34±0.24	70.4±8.1	72.9±52.1
Nonbloom mean ± SE		1.14±0.09	15.7±1.0	0.003±<0.001	0.006±0.001	1.35±1.26	47.8±12.4	5.0±3.8
Sta. ALOHA Jul–Aug (2008–2009) mean ± SE		1.13±0.08	53.3±21.3	0.005±0.001	0.010±0.005	1.29±0.65	70.1±12.5	6.8±2.3
Sta. ALOHA Sep–Jun (2008–2009) mean ± SE		1.01±0.06	13.8±2.0	0.006±0.002	0.014±0.003	2.07±0.41	42.2±3.9	8.2±1.2

* Bloom station.

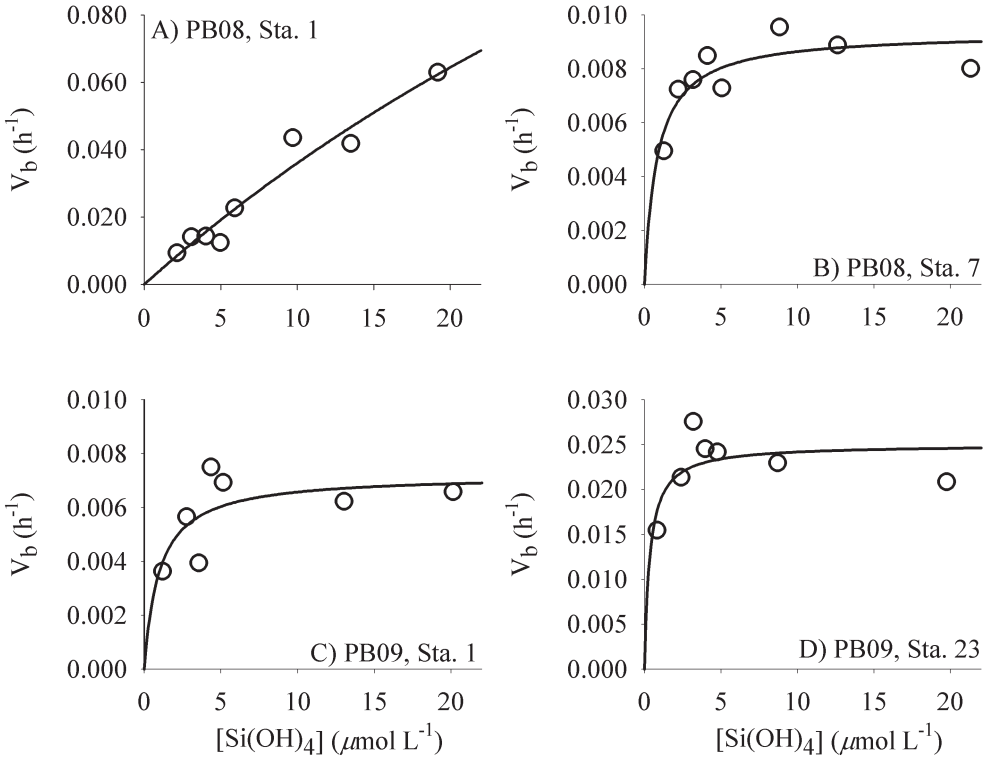

Fig. 2. Select full kinetic experiments from 59%I_0 depth showing the response of specific uptake (V_b) to increasing $[Si(OH)_4]$ from the (A, B) PB08 and (C, D) PB09 cruises. The curve fit is the Michaelis–Menten function. (A) The kinetic response to increasing $[Si(OH)_4]$ is linear and was the only such occurrence during the PB cruises. Linear uptake was also observed at some stations by Brzezinski et al. (1998) in this region. Note different V_b scales between panels.

which suggests that the finding of increases in V_{max} being proportionally similar to those in V_{amb} is robust. This finding is important for comparison of Si-uptake kinetic parameters between regions (*see* Discussion).

The calculation of V_{max}, like V_{amb}, normalizes gross silica production by total $[bSiO_2]$ (i.e., that associated with live cells and detrital fragments). Active Si uptake does not occur from silica associated with detritus, therefore, calculated values of V_{max} and V_{amb} underestimate the rates for living diatoms (Goering et al. 1973; Krause et al. 2010*a*). The PB08 bloom was sampled during a declining state (e.g., MODIS satellite data), so the detrital $bSiO_2$ at the bloom station may have been proportionally higher than at the nonbloom stations. This could explain the lack of significant differences in rates between the PB08 bloom station (V_{amb} and V_{max}) and some PB08 nonbloom stations (e.g., Sta. 14, 15). But in the PB09 bloom, the observed V_{amb} and V_{max} were $>$ 6-fold higher than at nonbloom stations (Table 2), which suggests a combination of more active diatoms and less influence of detrital $bSiO_2$ compared with the PB08 bloom. Unlike V_{max}, K_S is unaffected by the presence of siliceous detritus and more robust comparisons can be made between stations. The diatom bloom assemblages during both cruises tended to use silicic acid more efficiently than did nonbloom assemblages. The K_S values derived from eight-point kinetic experiments at the bloom stations sampled in PB08 and PB09 were 0.83 $\pm$ 0.30 μmol L^{-1} and 0.34 $\pm$ 0.24 μmol L^{-1}, respectively (Table 2), similar to the 0.55 μmol L^{-1} value observed by Brzezinski et al. (1998) for a summer diatom bloom in the NPSG. The nonbloom K_S values were similar during PB08 (1.33 $\pm$ 0.58 μmol L^{-1}) and PB09 (1.35 $\pm$ 1.26 μmol L^{-1}).

Like K_S, the ratio of Si uptake at ambient $[Si(OH)_4]$ to maximum uptake, $V_{amb}:V_{max}$, is not biased by detrital $bSiO_2$. $V_{amb}:V_{max}$ differed between bloom and nonbloom stations only during PB09. The ambient $[Si(OH)_4]$ in the PB08 and PB09 blooms supported uptake rates at 60.5% and 70.4% of V_{max}, respectively. Nonbloom diatom assemblages were operating at 58.1% of V_{max} during PB08 and 47.8% during PB09 (Table 2). The difference between nonbloom assemblages $V_{amb}:V_{max}$ between years is consistent with the average K_S being lower than ambient $[Si(OH)_4]$ during PB08, while the opposite was true for the nonbloom stations during PB09 (Table 2). The absolute difference between the mean values of $V_{amb}:V_{max}$ at the bloom and nonbloom station is conservative because of lower ambient $[Si(OH)_4]$ in bloom stations, which would lower V_{amb} and thus $V_{amb}:V_{max}$. If diatoms at the nonbloom stations experienced the same ambient $[Si(OH)_4]$ observed at the bloom stations, then the $V_{amb}:V_{max}$ for nonbloom diatoms under such conditions would decrease to 48.7% and 38.6% during PB08 and PB09, respectively (i.e., V_{amb} recalculated with nonbloom V_{max} and K_S values and bloom $[Si(OH)_4]$, *see* Eq. 1), such that bloom assemblages had

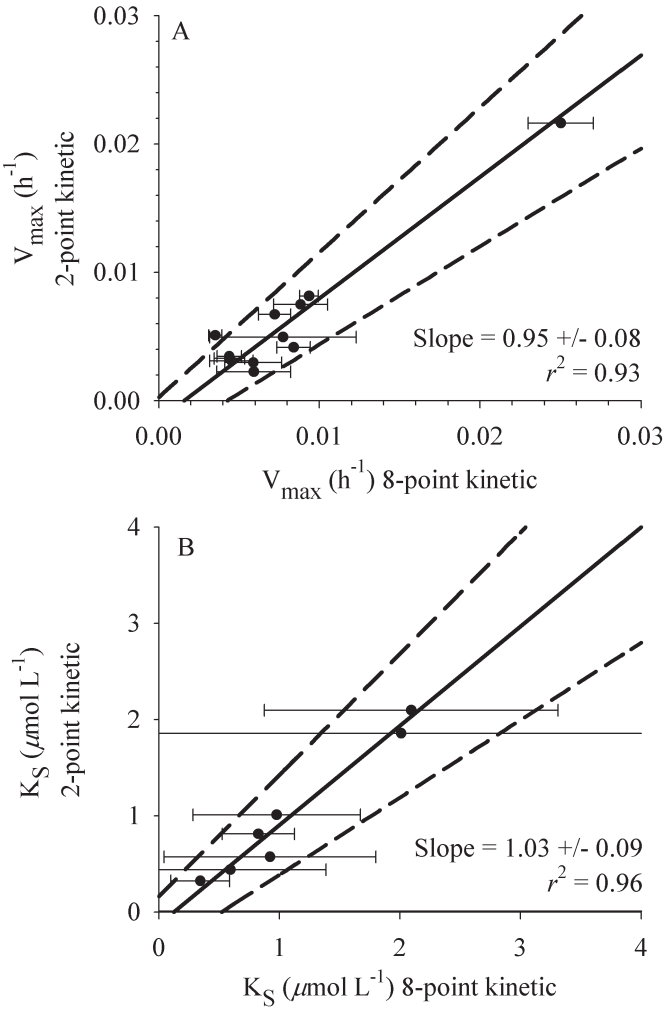

Fig. 3. Direct comparison of calculation methods for (A) V_{max} and (B) K_S. Eight-point kinetic experiments from both PB cruises were used. X-axis parameters and standard error (x-bars) were determined using an iterative nonlinear curve fitting algorithm (SigmaPlot 10.0©), the y-axis parameters were determined algebraically (Nelson et al. 2001) using only the V_b data from ambient $[Si(OH)_4]$ and + 20 μmol L^{-1} $[Si(OH)_4]$ samples. Model-II linear regressions, using a reduced major axis approach, are plotted (solid line) with the 95% CIs (dashed lines); the slope and SE are reported along with coefficient of determination (r^2).

relative uptake rates that were 12% (PB08) and 32% (PB09) closer to V_{max} than were nonbloom assemblages.

The initial slope of the Michaelis–Menten function, $V_{max}:K_S$, is proportional to the efficiency of nutrient use at low concentration (Healey 1980). The highest $V_{max}:K_S$ during the PB08 cruise was observed at a nonbloom station (Table 2). Even including this high value in the nonbloom station average, the PB08 bloom value, 11.3 (mmol Si L^{-1} $h)^{-1}$, was nearly twice the nonbloom station mean, 6.1 (mmol Si L^{-1} $h)^{-1}$ (Table 2). The nonbloom mean $V_{max}:K_S$ during the PB09 cruise was also low, 5.0 (mmol Si L^{-1} $h)^{-1}$, but the value in the bloom station, 72.9 (mmol Si L^{-1} $h)^{-1}$, was significantly higher than at any other station in both years (Table 2).

The depth profile of two-point kinetic experiments demonstrates how kinetic parameters change with attenuating light and relatively uniform $[Si(OH)_4]$. Very low $[bSiO_2]$ made it analytically challenging to detect a tracer signal at all profile depths, and profiles of three or more successful experiments were obtained at only three stations (Table 3). At these stations the dominant diatom proportion did not change significantly with depth (Table 3). At PB08 nonbloom Sta. 2, there was no vertical structure in any of the kinetic parameters. At depths shallower than 19%I_0, V_{amb} and V_{max} ranged from 0.004 h^{-1} to 0.006 h^{-1} and from 0.015 h^{-1} to 0.027 h^{-1}, respectively, while K_S ranged between 4.7 μmol L^{-1} to 7.1 μmol L^{-1}. Clear kinetic limitation was observed because diatoms at this station were only operating between 19% and 25% of V_{max} at ambient $[Si(OH)_4]$.

Vertical structure in kinetic parameters was observed at the other two stations. At Sta. 9 (PB08), V_{amb} and $V_{max}:K_S$ were both low and declined systematically with depth. Diatoms at this station were under clear kinetic limitation by ambient $[Si(OH)_4]$, such that $V_{amb}:V_{max}$ was only 16–29% (Table 3). At Sta. 22, within in the PB09 bloom region, two-point kinetic measurements were successfully made at 7 depths (Table 3; Fig. 4). V_{amb} and V_{max} at 59%I_0 were both elevated relative to nonbloom stations and there was a decline in both V_{amb} and V_{max} with depth (Fig. 4A). K_S was nearly constant with depth, ranging between $\sim$ 0.5 μmol L^{-1} and 0.7 μmol L^{-1} at all but the 19% I_0 isolume (Table 3). Ambient $[Si(OH)_4]$ allowed diatoms to operate between $\sim$ 40% and 70% of maximum uptake for all depths except for 6%I_0, where $V_{amb}:V_{max}$ was $\sim$ 114% (Table 3; Fig. 4B). $V_{max}:K_S$ also decreased with depth, driven mainly by changes in V_{max}; when $V_{max}:K_S$ at each light depth was normalized to $V_{max}:K_S$ at 100%I_0 (data not shown), the proportional decrease with depth was similar to that for irradiance with a Model-I regression of %I_0 vs. normalized %$V_{max}:K_S$ having a slope of 0.98 $\pm$ 0.14 ($\pm$ SE, $r^2 = 0.94$, $p < 0.01$).

Discussion

Kinetic and growth limitation of diatoms in the NPSG—Substrate limitation of diatom Si uptake has been observed at times in every ocean region studied to date (Brzezinski and Nelson 1996; Brzezinski et al. 1998; Leynaert et al. 2001). In the NASG and NPSG, $[Si(OH)_4]$ is rarely, if ever, high enough to support maximum Si-uptake rates (Brzezinski and Nelson 1996; Brzezinski et al. 1998; this study). $[Si(OH)_4]$ in the surface waters is generally < 2 μmol L^{-1}, but $[NO_3]$ and [SRP] are typically more than an order of magnitude lower. In the first study of Si kinetics in the open ocean (Brzezinski and Nelson 1996), it was expected that limitation of diatoms by a nutrient other than Si would decouple Si uptake from its rate of supply, because diatom biomass and Si uptake would be controlled by the supply of the limiting nutrient, thereby allowing ambient $[Si(OH)_4]$ to increase above that needed to meet diatom demand. In contrast, comparison of the kinetics of Si use with ambient $[Si(OH)_4]$ in the NASG led Brzezinski and Nelson (1996) to conclude that high $[Si(OH)_4]$ relative to the low N and P

Table 3. Two-point kinetic experiment results with depth along with temperature at the depth of collection, concentrations of dissolved silicate and biogenic silica, diatom abundance, and the dominant diatom (with its percent abundance relative to the total diatom community). For information on relative error estimates when using the two-point kinetic method, *see* Results.

Cruise	Station	%I_0 (Depth m)	Temp (°C)	[$Si(OH)_4$] (μmol L^{-1})	[$bSiO_2$] (nmol Si L^{-1})	V_{amb} (h^{-1})	V_{max} (h^{-1})	K_s (μmol L^{-1})	$V_{amb}:V_{max}$ (%)	$V_{max}:K_s$ (mmol L^{-1} $h)^{-1}$	Diatoms (cells L^{-1})	Dominant diatom (%)
PB08	2	100(4)	22.8	1.59	31.7	0.006	0.027	5.84	21.4	4.5	166	*H. hauckii* (97.6)
		59(15)	22.8	1.60	33.3	0.006	0.024	4.73	25.3	5.1	331	*H. hauckii* (48.3)
		31(32)	21.8	1.58	48.9*	0.004	0.015	5.23	23.2	2.8	353	*H. hauckii* (91.2)
		19(46)	21.1	1.62	20.8	0.004	0.023	7.12	18.5	3.2	192	*H. hauckii* (43.2)
PB08	9	59(18)	21.3	1.55	40.4	0.003	0.009	3.86	28.6	2.4	191	*H. hauckii* (84.8)
		31(33)	21.2	1.53	67.5	0.002	0.007	3.98	27.8	1.6	170	*H. hauckii* (76.5)
		10(66)	18.7	2.01	60.0	0.001	0.006	10.57	16.0	0.5	64	*H. hauckii* (40.6)
PB09	22†	100(4)	25.9	0.86	46.1*	0.021	0.035	0.57	60.1	61.0	3270	*M. woodiana* (97.2)
		59(11)	25.8	0.88	64.1*	0.018	0.032	0.69	56.1	46.6	5183	*M. woodiana* (98.7)
		31(23)	25.7	0.89	74.0	0.010	0.016	0.45	66.4	34.7	9620	*M. woodiana* (99.8)
		19(33)	25.6	0.89	57.2	0.010	0.024	1.37	39.2	17.8	8120	*M. woodiana* (98.5)
		10(45)	23.8	1.06	153.1	0.004	0.006	0.77	57.8	8.1	23,820	*M. woodiana* (99.0)
		6.0(54)	22.5	1.26	57.2	0.002	0.001	—	114.3	—	3940	*M. woodiana* (99.0)
		3.4(65)	21.8	1.33	19.0	0.002	0.002	0.57	70.0	4.0	500	*M. woodiana* (100)

* Denotes $bSiO_2$ in the > 10-μm size-fraction opposed to > 0.6-μm (all other values).
† Bloom station.

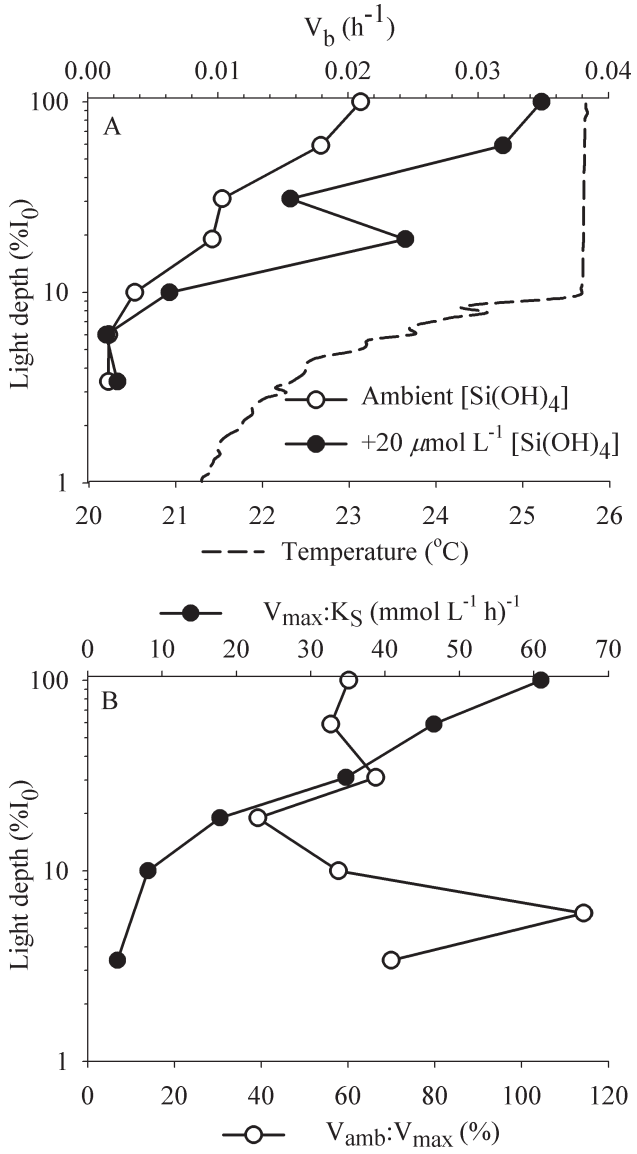

Fig. 4. Assessment of kinetic responses within the euphotic zone in the PB09 bloom (Sta. 22). (A) Shows the decline in V_{amb} and V_{max} (~ 20 μmol L^{-1} [$Si(OH)_4$]) with decreasing %I_0. The temperature profile shows the light depths relative to the thermal structure. (B) The efficiency of uptake at low [$Si(OH)_4$] ($V_{max}:K_S$, circles, top scale) and the operational percentage of V_{max} supported by ambient [$Si(OH)_4$] ($V_{amb}:V_{max}$, squares, bottom scale) as a function of %I_0.

was driven by inefficient Si-uptake kinetics, rather than an excess of $Si(OH)_4$ supply relative to diatom demand. Our results support that general view in the NPSG.

Combining all kinetic data from the NPSG (Brzezinski et al. 1998, 2011; this study) clarifies the extent of kinetic limitation of Si uptake in this system. These studies collectively performed 56 experiments and 52 showed that ambient [$Si(OH)_4$] was insufficient to support maximum Si uptake with the average V_{amb} restricted to 42% ± 3% (SE) of V_{max}. These experiments were conducted at 25 distinct locations in the NPSG and suggest that kinetic limitation of Si uptake is not only temporally persistent, but spatially

widespread, from the gyre interior near Sta. ALOHA to the subtropical front boundary.

There is clear evidence for kinetic limitation in the NPSG, but it is more difficult to assess whether the growth rates of diatoms in these experiments were limited by low $[Si(OH)_4]$. Diatoms thin their frustules and lower Si-uptake rates in response to suboptimal $[Si(OH)_4]$. They sustain a close match between cellular demand for Si and its rate of acquisition, such that decreases in $[Si(OH)_4]$ have only a minor effect on growth rate, so long as the capacity of cells to reduce their cellular Si levels is not exceeded. Once that happens, Si limitation of diatom growth ensues. Diatoms in culture can alter their Si content up to a factor of four (*see* review by Martin-Jézéquel et al. 2000); therefore, values of $V_{amb}:V_{max} < 25\%$ imply limitation of diatom growth. This ratio is robust against factors that can alter silicification. The Si content of diatoms can change in response to limitation of growth rate by factors aside from Si (e.g., N, P, light; Claquin et al. 2002). The specific mechanism for changing Si content under these conditions is an increase in the duration of cell cycle phases associated with Si uptake. By this mechanism, cells increase cellular Si levels by taking up $Si(OH)_4$ for longer periods rather than by changing the rate of uptake; hence, the specific affinity for Si uptake does not change (Brzezinski et al. 1990; Claquin et al. 2002). Changes in cell size or shifts in the number of Si transporters on the cell surface may alter V_{max}, but because V_{amb} and V_{max} are inherently coupled through the Michaelis–Menten function, shifts in V_{max} induce proportional shifts in V_{amb} and $V_{amb}:V_{max}$ is unchanged (*see* Results). Therefore, the use of $V_{amb}:V_{max}$ to assess potential Si limitation of growth is a reasonable diagnostic, with the uncertainty being the analytical uncertainty of the measurement (e.g., ± 8%). The mean value of $V_{amb}:V_{max}$ in the NPSG, 42%, exceeds the threshold of 25%, which suggests that, on average, $[Si(OH)_4]$ does not limit diatom growth in this gyre; however, exceptions occur (Tables 2, 3). Substrate limitation of Si uptake is more severe in the NASG (mean $V_{amb}:V_{max}$ = 26%, see below), such that limitation of diatom growth rate by Si appears to be a strong possibility (Brzezinski and Nelson 1996).

Bloom development and kinetic efficiency of Si uptake at low substrate—Our data set allows a test of Brzezinski et al. 's (1998) hypothesis that high kinetic efficiency for Si uptake at low substrate facilitates the net accumulation of diatom biomass in diatom blooms in oligotrophic waters. It appears unlikely that diatom growth and cell division was limited by $[Si(OH)_4]$; therefore, high kinetic efficiency does not appear to be facilitative for diatom blooms.

For both cruises, multiple lines of evidence suggested that diatoms at the bloom stations used $Si(OH)_4$ more efficiently than those outside of blooms. The two parameters not affected by the presence of detrital $bSiO_2$, K_S and $V_{amb}:V_{max}$, both suggest higher kinetic efficiency in blooms; K_S values tend to be lower and $V_{amb}:V_{max}$ values tend to be higher, even at reduced $[Si(OH)_4]$, relative to nonbloom means (Tables 2, 3). The diagnostic of Si-uptake efficiency at low substrate concentration, $V_{max}:K_S$, shows a much broader range in the NPSG than in the NASG or

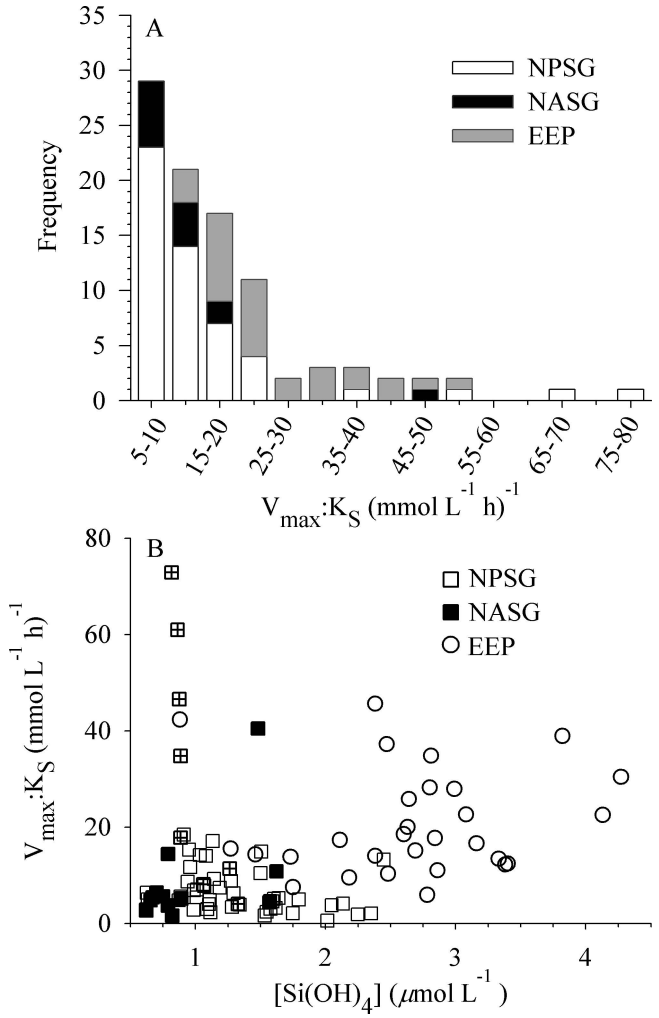

Fig. 5. (A) Frequency histogram of $V_{max}:K_S$ (binned in 5 [mmol L^{-1} $h]^{-1}$ intervals) and (B) $V_{max}:K_S$ vs. $[Si(OH)_4]$ for kinetic experiments from the NPSG (open squares, n = 52, open and crossed squares indicate PB08 and PB09 blooms; this study; Brzezinski et al. 1998, 2011), NASG (closed squares, n = 13; Brzezinski and Nelson 1996; Krause et al. 2010*b*; J. W. Krause and D. M. Nelson unpubl.), and EEP (open circles, n = 29; Brzezinski et al. 2008). Note—the total NSPG data set was reported as 56 experiments (*see* Discussion) but in four two-point kinetic experiments $V_{amb} \approx V_{max}$; under such circumstances, K_S cannot be determined. The four highest NPSG values (35–73 [mmol L^{-1} $h]^{-1}$) are all from the PB09 bloom (i.e., Sta. 22 and 23).

eastern equatorial Pacific (EEP, Fig. 5) and $V_{max}:K_S$ was generally higher in blooms stations vs. the corresponding nonbloom means (Tables 2, 3; Fig. 5). The values of $V_{max}:K_S$ within the PB09 bloom at Sta. 22 and 23, 61.0 and 72.9 (mmol Si L^{-1} $h)^{-1}$ (Tables 2, 3), are the highest ever measured in the open ocean or in coastal regions, exceeding the previous maximum of > 55 (mmol Si L^{-1} $h)^{-1}$ (see compilation of prior data Brzezinski et al. 2008), which makes those diatom assemblages the most kinetically efficient observed to date (Fig. 5). High kinetic efficiency for Si uptake optimizes biomass yield in a bloom, where there is no input of $[Si(OH)_4]$ into the euphotic zone, by allowing $bSiO_2$ accumulation without inducing secondary

growth limitation from the resulting draw-down in the already low [$Si(OH)_4$].

The PB08 bloom is an exception to these trends, with values of V_{amb} and V_{max} within the bloom region being similar to some nonbloom stations. During the PB08 bloom, the diatom community was likely in a state of decline at the time of sampling because the MODIS-observed ocean color in the area faded while the ship was en route to the bloom area (data not shown). This is consistent with the higher V_{amb} observed at some stations outside the bloom (Table 2), which could be a result of higher proportion of detrital $bSiO_2$ or declining physiological rates within the former bloom region.

The indirect role of light in regulating Si uptake—The kinetics of Si uptake were coupled with light availability. V_{amb}, V_{max}, and $V_{max}:K_S$ declined with irradiance at two of the three stations where data on changes in these parameters with depth were obtained. At Sta. 22 during PB09, where we have the most detailed profile (Table 3; Fig. 4), light and the efficiency of uptake at lower substrate availability were strongly coupled. Values of $V_{max}:K_S$ at each depth normalized to the ratio measured at the shallowest depth were strongly correlated with the fraction of surface irradiance present at each depth (slope = 0.98 ± 0.14). This trend did not appear to be the result of a change in species composition with depth because the relative abundance of *M. woodiana* throughout the euphotic zone was nearly constant (Table 3).

A role for light in regulating field-population Si kinetics in the open ocean has not been directly observed. The transport and polymerization of silicic acid by diatoms requires adenosine triphosphate (Blank and Sullivan 1979) and an array of organic compounds (Kröger and Poulsen 2008), and the process has some coupling to photosynthesis. But the decline in Si transport due to darkening is slow (> 6 h; Blank and Sullivan 1979), which may account for the observation that average rates of silica production during the day and night are often found to be similar in field studies (Chisholm et al. 1978; Nelson and Brzezinski 1997). On shorter timescales, Kudela (2008) demonstrated that Si uptake in recently upwelled waters in Monterey Bay increased and saturated in response to increasing irradiances; however, this saturation closely mirrored the response to N uptake, which suggests the coupling of Si and light was indirect.

In our study, the coupling of light and Si uptake may be mediated by the effects of light on N metabolism. Using a theoretical model, Geider et al. (1996) suggested that the switch from high to low irradiance shifts the critical N : P demand for phytoplankton. This is because the components of light harvesting and photosynthetic electron-transfer complexes have higher N requirements, relative to P, and an investment in light harvesting complexes is necessary to maximize photon capture at low irradiance. If the concentration of inorganic N is uniformly low and growth-limiting in the euphotic zone, then cells at higher irradiance can meet their necessary N quota for cell division faster than cells at low irradiances. In this case, vertical trends in Si uptake (V_b) would simply track changes in depth related to shifts in division rates and, because of the strong proportional coupling between V_{amb} and V_{max} (*see* Results), the same would be true for vertical trends in V_{max}.

Under such circumstances, the accumulation of diatom biomass is expected to be localized in the upper euphotic zone where maximum division rates and Si-uptake efficiency are predicted to co-occur. During the PB cruises (J. W. Krause and M. A. Brzezinski unpubl.) and also at Sta. ALOHA (Brzezinski et al. 2011), the highest [$bSiO_2$] and V_b were observed at depths shallower than ~ 50 m (i.e., the well-lit section of the water column). This pattern of increased diatom biomass in the upper 50 m is also consistent with observations in many different studies of summer diatom blooms in this region (Brzezinski et al. 1998; Dore et al. 2008; Villareal et al. 2011) and also with Venrick's (1988) classification of the bloom diatoms in our study (*H. hauckii* and *M. woodiana*) as upper-water column groups in the NPSG.

Diatom community composition and enhanced kinetic efficiency—Kinetic parameters measured in field studies are composite values for all diatoms in a particular sample, with the contribution of the uptake kinetics of any single species being driven by its abundance, growth rate, and silica content. Although there are no published reports of Si per cell for *M. woodiana* or *H. hauckii* and *Rhizosolenia* spp. with endosymbionts, we can estimate Si content using a biovolume scaling approach (Conley et al. 1989). For *M. woodiana,* we assume a prolate-sphere shape and use previously published cell-dimension information (5-μm width, 25-μm length; *see* Blueford et al. 1990) to estimate a biovolume of 327 μm^3, which corresponds to a Si quota of 0.13 pmol Si $cell^{-1}$. Similarly, for *Rhizosolenia* spp., we use the median dimensions reported by Ferrario et al. (1995) for *Rhizosolenia clevei* var. *communis* Sundstrom in the North Pacific (width 20 μm, length 400 μm) and assume a cylinder shape, which yields a biovolume of 1.25×10^5 μm^3 and a 30.2-pmol Si $cell^{-1}$ Si content. And for *H. hauckii,* we use an average of the reported biovolumes for 19 *Hemiaulus* cells with endosymbionts in Foster et al. (2011), 5878 μm^3, which yields 1.86 pmol Si $cell^{-1}$. Multiplying the Si content estimates by the abundance allows for an estimate of the contribution for each diatom to the $bSiO_2$ concentration.

During the PB08 bloom, the rank-order contribution to the total $bSiO_2$ concentration at the 59% light depth was *H. hauckii* (2.6 nmol Si L^{-1}), *Rhizosolenia* spp. (2.4 nmol Si L^{-1}), and *M. woodiana* (< 0.1 nmol Si L^{-1}). In culture, *H. hauckii* (T. A. Villareal unpubl.) and *Rhizosolenia* spp. (Villareal 1990) with endosymbionts have been observed to grow at 0.8 divisions d^{-1}. Because of the disparity between the contribution to total [$bSiO_2$] by *M. woodiana* vs. the larger diatoms, *M. woodiana*'s growth rate would have to be about 25-fold higher than that of *H. hauckii* and *Rhizosolenia* spp. in order for them to dominate community silica production. Such a growth rate seems unlikely considering that the net growth rates expressed by *H. hauckii* resulted in their being 10-fold more abundant than *M. woodiana*. Additionally, although *H. hauckii* and *Rhizosolenia* spp. show similar division rates in cultures,

the net growth rates expressed by *H. hauckii* in the PB08 bloom resulted in a 20-fold higher abundance than *Rhizosolenia* spp. Thus, we conclude that *H. hauckii* likely dominated community silica production in this bloom, and thus dominated the diatom production of organic matter.

The overwhelming numerical dominance by *M. woodiana* in the PB09 bloom would suggest a large contribution by this group to total Si production. Using the same approach as above, we can examine whether or not *H. hauckii* and *Rhizosolenia* may have had similar contributions to community uptake as *M. woodiana*. We averaged the diatom contribution at both Sta. 22 and 23, and also with depth, to derive the rank-order contribution for each diatom group to total [$bSiO_2$]: *Rhizosolenia* spp. (1.3 nmol Si L^{-1}), *M. woodiana* (1.1 nmol Si L^{-1}), and *H. hauckii* (< 0.1 nmol Si L^{-1}). Given the low contribution by *H. hauckii* to total $bSiO_2$, ~ 12-fold higher growth rates would be necessary to dominate community silica production, which seems unlikely. With nearly equal contributions to total [$bSiO_2$] by *Rhizosolenia* spp. and *M. woodiana*, it would suggest that these two diatoms may have had similar contributions to silica production. However, the net growth rates expressed by *M. woodiana* in this bloom were sufficient to increase their abundance by three orders of magnitude above nonbloom abundances, whereas the net growth rates observed by *Rhizosolenia* spp. in this bloom resulted in an order of magnitude abundance increase vs. nonbloom stations. Such a difference in net growth rates between smaller pennate diatoms (e.g., *M. woodiana*) and larger centrics (e.g., *Rhizosolenia*) would be consistent with the results of Furnas (1991), who observed that small pennates grew faster in near-surface in situ diffusion chambers in a tropical environment than diatoms from the *Rhizosolenia* spp. diatoms. Thus, we conclude that *M. woodiana* dominated community silica production during the PB09 bloom.

All other factors being equal, a direct comparison of the kinetics between blooms also supports the interpretation that different diatoms dominated silica production during each bloom. $V_{amb}:V_{max}$ observed at the PB09 bloom station was ~ 5% higher than during the PB08 bloom, despite [$Si(OH)_4$] in the PB08 bloom being 50% higher than in the PB09 bloom. Assuming Si-kinetic parameters are conserved among species, if the same diatom group dominated Si uptake in both blooms, then the combined effects of the increase in V_{max} and the lower [$Si(OH)_4$] would have lowered $V_{amb}:V_{max}$ in the PB09 bloom relative to that observed during the PB08 bloom (*see* Eqs. 1, 2); this did not occur (Table 2). This evidence suggests the numerical dominance by *M. woodiana* in the PB09 bloom was also a biogeochemical shift to their dominance of community Si uptake. Such a confirmation is important in light of a recent analysis demonstrating that large but numerically rare diatoms (i.e., $\leq$ 10% of the total diatom abundance) may be responsible for up to 40% of community Si uptake in the EEP (Krause et al. 2010*a*). This also suggests that, in the NPSG, dominance of diatom silica and organic matter production during blooms can switch between diatom species that have or do not have diazotrophic endosymbionts.

The diatom community at the PB09 bloom stations possessed the highest Si-uptake efficiency at low [$Si(OH)_4$] observed in any oceanic habitat to date (Fig. 5). The increased $V_{max}:K_S$ helps to explain how *M. woodiana* accumulated $bSiO_2$ in the upper water column without additional input of $Si(OH)_4$. The K_S value observed in this bloom (0.34 μmol L^{-1}) is also the lowest observed in the combined 94 kinetic experiments reported from the EEP, NASG, and NPSG (data from Figs. 5, 6) and supports the interpretation that increased efficiency of uptake helps diatoms stave off potential growth limitation by Si availability when ambient [$Si(OH)_4$] is lowered.

Implications for Si-uptake kinetics in oligotrophic regions—The global data set on Si-uptake kinetics in oligotrophic systems is sufficiently large to allow global trends to be evaluated. Combining data from the NPSG, the EEP, and the NASG, there have been 94 estimates of Si-uptake kinetic parameters. In the majority of cases, the measured values of $V_{amb}:V_{max}$ exceed the threshold value of 25% (plus the analytical uncertainty) that would be indicative of Si-limited growth, but there are strong regional differences. In the EEP, all of the estimates $V_{amb}:V_{max}$ exceed the threshold of 25% that would suggest growth-rate limitation by Si (Brzezinski et al. 2008). Potential Si limitation of growth is more prevalent in the subtropical gyres, where 21% of the values of $V_{amb}:V_{max}$ from the NPSG are $< 25\%$, with 69% being below this threshold in the NASG. These trends parallel those in [$Si(OH)_4$] among regions; average silicic acid concentrations range from 2.67 $\pm$ 0.12 μmol L^{-1} in the EEP to 1.30 $\pm$ 0.06 μmol L^{-1} in the NPSG and 0.92 $\pm$ 0.10 μmol L^{-1} in the NASG (Fig. 6C). But the trends in K_S do not follow a simple inverse trend with [$Si(OH)_4$] that would be expected if diatoms simply adapted to low concentrations by lowering K_S. The lowest average value of K_S, 1.7 $\pm$ 0.1 μmol L^{-1}, was observed in the EEP, followed by 3.5 $\pm$ 0.5 μmol L^{-1} NASG and 5.4 $\pm$ 1.8 μmol L^{-1} in the NPSG. The relationship between Si stress and Si-uptake kinetics is more complex.

To further examine how susceptibility to growth limitation by Si is related to Si-uptake kinetics trends in $V_{amb}:V_{max}$ relative to changes in K_S, the Michaelis–Menten function (Eq. 1) was rearranged as:

$$\frac{V}{V_{max}} = \frac{[Si(OH)_4]}{K_S + [Si(OH)_4]} \quad (2)$$

Equation 2 demonstrates that $V_{amb}:V_{max}$ increases at higher [$Si(OH)_4$] and decreases when K_S increases; therefore, for a given [$Si(OH)_4$], a unique curve depicts the relationship between the percentage $V_{amb}:V_{max}$ and K_S (Fig. 6A). Considering the mean [$Si(OH)_4$] for each region, Fig. 6B predicts that Si limitation of growth would be avoided for assemblages with K_S values < 8.0 μmol L^{-1}, < 3.9 μmol L^{-1}, and < 2.8 μmol L^{-1} for the EEP, NPSG, and NASG, respectively. Figure 6B shows that the reason behind the higher proportion of the experiments falling below the $V_{amb}:V_{max}$ threshold of 25% in the NASG, compared with the NPSG, is that the low ambient [$Si(OH)_4$] in the NASG

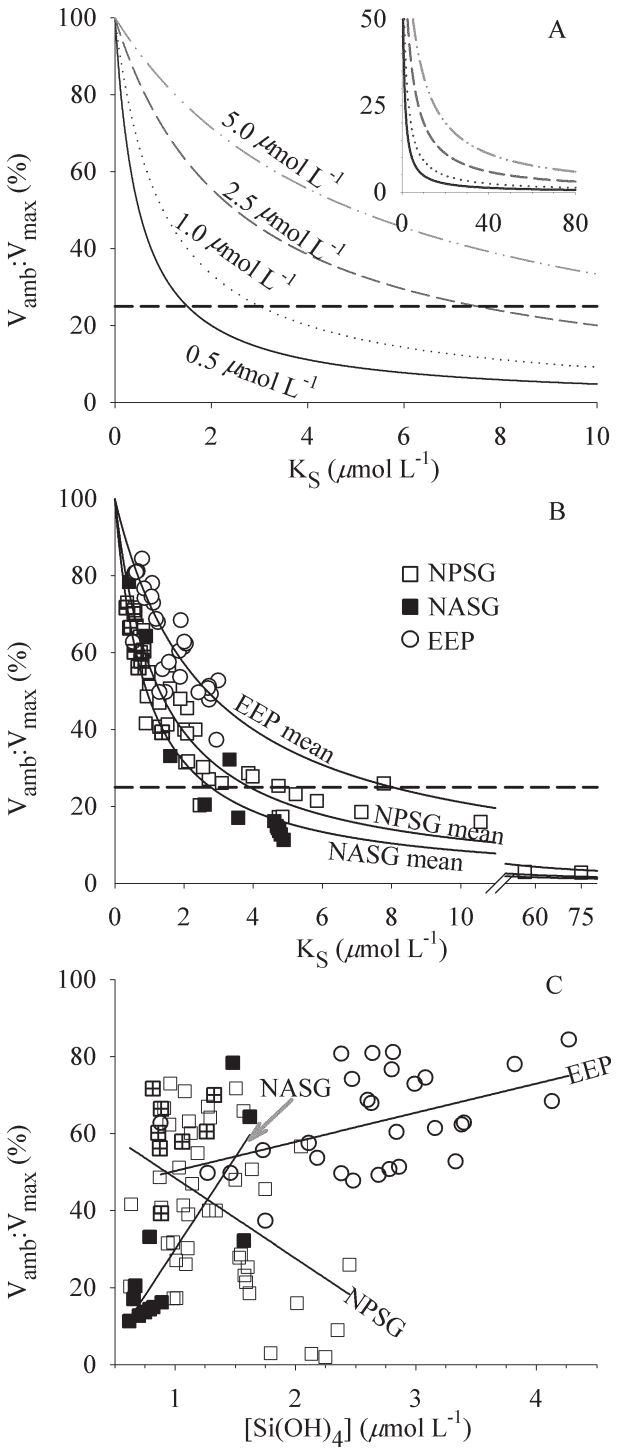

Fig. 6. Comparison of kinetic parameters in three open-ocean regions. (A, B) The operational percentage of V_{max} by diatoms under ambient $[Si(OH)_4]$ ($V_{amb}:V_{max}$) as a function of K_S. (A) Shows the theoretical relationship between $V_{amb}:V_{max}$ and K_S for different substrate availability (curves labeled by $[Si(OH)_4]$) depicted by Eq. 2; the inset shows the same set of curves but the y-axis is truncated and the x-axis is increased nearly an order of magnitude. (B) Shows field data from three open-ocean regions: NPSG, NASG, and EEP. For visualization, the x-axis is broken to show the highest K_S values measured (56.5 μmol L^{-1}, Brzezinski et al. 1998; 75.0 μmol L^{-1}, this study) but omits two intermediate K_S values (15.5 μmol L^{-1} and 25.9 μmol L^{-1}, Brzezinski et al. 1998); K_S values > 5 μmol L^{-1} were only observed in the NPSG. Curves depicted are based on the mean $[Si(OH)_4]$ for the data in each region. The dashed line (A, B) denotes the criterion where diatom growth may be limited by ambient $[Si(OH)_4]$. (C) $V_{amb}:V_{max}$ as a function of $[Si(OH)_4]$ with linear regression fits for each region. Data source is listed in Fig. 5 and regional symbols are the same in (B) and (C), with PB cruise blooms depicted as crossed squares (as in Fig. 5).

demands a proportionally lower K_S to exceed the threshold, compared with the NPSG. So despite the lower average K_S in the NASG compared with that in the NPSG, a higher proportion of experiments from NASG exhibit a level of Si stress consistent with growth limitation by Si.

This analysis requires a revision to the argument of Brzezinski and Nelson (1996) that the potential for growth limitation by Si in oligotrophic systems is predominantly a function of kinetic inefficiency. Our analysis shows that within a region the least kinetically efficient assemblages experience the highest level of Si stress, but the adaptive advantage of a given value of K_S must take into account regional differences in $[Si(OH)_4]$. Regional differences are further illustrated by the relationship between $V_{amb}:V_{max}$ and $[Si(OH)_4]$. In both the NASG and the EEP, $V_{amb}:V_{max}$ is positively correlated with $[Si(OH)_4]$, although the slope of the relationship is stronger in the NASG (Fig. 6C). The relationship for the NSPG is different, with $V_{amb}:V_{max}$ decreasing with increasing $[Si(OH)_4]$ (Fig. 6C), which suggests that in this region the susceptibility to growth limitation by Si appears driven by kinetic inefficiency rather than low $[Si(OH)_4]$. Therefore, Brzezinski and Nelson's (1996) argument about potential growth limitation in the NASG due to kinetic inefficiency appears to be more appropriate in the NPSG.

In summary, we confirm previous results that diatom Si uptake is limited by low ambient $[Si(OH)_4]$ in the NPSG. Combining all available studies, conditions where diatoms were potentially growth-limited by ambient $[Si(OH)_4]$ were observed in only 21% of experiments in the NPSG, which is much less frequent than in the NASG (i.e., 69%). The regional difference is explained by diatoms in the NASG experiencing lower ambient $[Si(OH)_4]$ without a corresponding decline in K_S to maintain $V_{amb}:V_{max}$ in the range observed in the NPSG. Enhanced kinetic efficiency tended to be observed within diatom blooms relative to nonbloom regions. Vertical profiles of kinetic experiments demonstrate the indirect coupling of light and Si uptake, potentially through N-limited diatoms having faster division rates at higher irradiance. The diatom community observed in the PB09 bloom had the most efficient uptake systems for $Si(OH)_4$ observed anywhere in the ocean to date, and the community Si uptake was likely driven by responses from *M. woodiana*. Our data suggest that increased kinetic efficiency leads to the accumulation of diatom $bSiO_2$ by continued draw-down of the already low $[Si(OH)_4]$ without the need for additional input of $Si(OH)_4$ into the system, and that more efficient kinetics maximizes the amount of new biomass created before growth limitation by Si would ensue.

Acknowledgments

We thank J. Jones, E. Allman, C. Beucher, C. Brown, V. Franck, J. Goodman, A. Pyle, K. Rogers, K. Swanson, and S. Vega for logistical and technical assistance, M. Church and S. Duhamel for data access, the Captain, resident technicians, and crew of the R/V *Kilo Moana* for assistance at sea and the anonymous reviewers for their insightful comments. This work was funded by National Science Foundation Ocean Sciences grants OCE-0648130 awarded to MAB, and OCE-0726726 and OCE-0094591 awarded to TAV.

References

Blank, G., and C. Sullivan. 1979. Diatom mineralization of silicic acid III. $Si(OH)_4$ binding and light dependent transport in *Nitzschia angularis*. Arch. Microbiol. **123:** 157–164, doi:10.1007/BF00446815

Blueford, J. R., J. J. Gonzales, and K. Vanscoy. 1990. Comparing radiolarian and diatom diversity and abundance from the Northeast Pacific. Mar. Micropaleontol. **15:** 219–232, doi:10.1016/0377-8398(90)90012-B

Brzezinski, M. A., C. Dumousseaud, J. W. Krause, C. I. Measures, and D. M. Nelson. 2008. Iron and silicic acid concentrations together regulate Si uptake in the equatorial Pacific Ocean. Limnol. Oceanogr. **53:** 875–889, doi:10.4319/lo.2008.53.3.0875

———, J. W. Krause, M. J. Church, D. M. Karl, B. Li, J. L. Jones, and B. Updyke. 2011. The annual silica cycle of the oligotrophic North Pacific ocean. Deep-Sea Res. I **58:** 988–1001, doi:10.1016/j.dsr.2011.08.001

———, and D. M. Nelson. 1995. The annual silica cycle in the Sargasso Sea near Bermuda. Deep-Sea Res. I **42:** 1215–1237.

———, and ———. 1996. Chronic substrate limitation of silicic acid uptake rates in the western Sargasso Sea. Deep-Sea Res. II **43:** 437–453.

———, R. J. Olson, and S. W. Chisholm. 1990. Silicon availability and cell-cycle progression in marine diatoms. Mar. Ecol. Prog. Ser. **67:** 83–96, doi:10.3354/meps067083

———, and D. R. Phillips. 1997. Evaluation of Si-32 as a tracer for measuring silica production rates in marine waters. Limnol. Oceanogr. **42:** 856–865, doi:10.4319/lo.1997.42.5.0856

———, T. A. Villareal, and F. Lipschultz. 1998. Silica production and the contribution of diatoms to new and primary production in the central North Pacific. Mar Ecol. Prog. Ser. **167:** 89–104, doi:10.3354/meps167089

Chisholm, S. W., F. Azam, and R. W. Eppley. 1978. Silicic acid incorporation in marine diatoms on light–dark cycles: Use as an assay for phased cell division. Limnol. Oceanogr. **23:** 518–529, doi:10.4319/lo.1978.23.3.0518

Church, M. J., C. Mahaffey, R. M. Letelier, R. Lukas, J. P. Zehr, and D. M. Karl. 2009. Physical forcing of nitrogen fixation and diazotroph community structure in the North Pacific subtropical gyre. Glob. Biogeochem. Cycles **23:** GB2020, doi:10.1029/2008GB003418

Claquin, P., V. Martin-Jézéquel, J. C. Kromkamp, M. J. W. Veldhuis, and G. W. Kraay. 2002. Uncoupling of silicon compared with carbon and nitrogen metabolisms and the role of the cell cycle in continuous cultures of *Thalassiosira pseudonana* (Bacillariophyceae) under light, nitrogen, and phosphorous control. J. Phycol. **38:** 922–930, doi:10.1046/j.1529-8817.2002.t01-1-01220.x

Conley, D. J., S. S. Kilham, and E. Theriot. 1989. Differences in silica content between marine and fresh-water diatoms. Limnol. Oceanogr. **34:** 205–213, doi:10.4319/lo.1989.34.1.0205

Dore, J. E., R. M. Letelier, M. J. Church, R. Lukas, and D. M. Karl. 2008. Summer phytoplankton blooms in the oligotrophic North Pacific Subtropical Gyre: Historical perspective and recent observations. Prog. Oceanogr. **76:** 2–38, doi:10.1016/j.pocean.2007.10.002

Duhamel, S., K. M. Björkman, F. V. Wambeke, T. Moutin, and D. M. Karl. 2011. Characterization of alkaline phosphatase activity in the North and South Pacific Subtropical Gyres: Implications for phosphorus cycling. Limnol. Oceanogr. **56:** 1244–1254, doi:10.4319/lo.2011.56.4.1244

———, S. T. Dyhrman, and D. M. Karl. 2010. Alkaline phosphatase activity and regulation in the North Pacific Subtropical Gyre. Limnol. Oceanogr. **55:** 1414–1425, doi:10.4319/lo.2010.55.3.1414

Ferrario, M. E., V. Villafañe, W. Helbling, and O. Holm Hansen. 1995. The occurrence of the symbiont *Richelia* in *Rhizosolenia* and *Hemiaulus* in the North Pacific. Rev. Bras. Biol. **55:** 439–443.

Foster, R. A., M. M. M. Kuypers, T. Vagner, R. W. Paerl, N. Musat, and J. P. Zehr. 2011. Nitrogen fixation and transfer in open ocean diatom–cyanobacterial symbioses. Int. Soc. Microb. Ecol. J. **5:** 1484–1493.

———, and J. P. Zehr. 2006. Characterization of diatom–cyanobacteria symbioses on the basis of nifH, hetR and 16S rRNA sequences. Environ. Microb. **8:** 1913–1925, doi:10.1111/j.1462-2920.2006.01068.x

Furnas, M. J. 1991. Net in situ growth rates of phytoplankton in an oligotrophic, tropical shelf ecosystem. Limnol. Oceanogr. **36:** 13–29, doi:10.4319/lo.1991.36.1.0013

Geider, R. J., H. L. Macintyre, and T. M. Kana. 1996. A dynamic model of photoadaptation in phytoplankton. Limnol. Oceanogr. **41:** 1–15, doi:10.4319/lo.1996.41.1.0001

Goering, J. J., D. M. Nelson, and J. A. Carter. 1973. Silicic acid uptake by natural populations of marine phytoplankton. Deep-Sea Res. **20:** 777–789.

Healey, F. P. 1980. Slope of the Monod equation as an indicator of advantage in nutrient competition. Microbial Ecology **5:** 281–286, doi:10.1007/BF02020335

Krause, J. W., M. A. Brzezinski, and J. L. Jones. 2011. Application of low level beta counting of ^{32}Si for the measurement of silica production rates in aquatic environments. Mar. Chem. **127:** 40–47, doi:10.1016/j.marchem.2011.07.001

———, and others. 2010*a*. The effects of biogenic silica detritus, zooplankton grazing, and diatom size structure on silicon cycling in the euphotic zone of the eastern equatorial Pacific. Limnol. Oceanogr. **55:** 2608–2622, doi:10.4319/lo.2010.55.6.2608

———, D. M. Nelson, and M. W. Lomas. 2009. Biogeochemical responses to late-winter storms in the Sargasso Sea. II. Increased rates of biogenic silica production and export. Deep-Sea Res. I **56:** 861–874, doi:10.1016/j.dsr.2009.01.002

———, ———, and ———. 2010*b*. Production, dissolution, accumulation and potential export of biogenic silica in a Sargasso Sea mode-water eddy. Limnol. Oceanogr. **55:** 569–579, doi:10.4319/lo.2009.55.2.0569

Kröger, N., and N. Poulsen. 2008. Diatoms—from cell wall biogenesis to nanotechnology. Ann. Rev. Genet. **42:** 83–107, doi:10.1146/annurev.genet.41.110306.130109

Kudela, R. M. 2008. Silicon : Nitrogen interactions in the marine environment, p. 1561–1598. *In* D. Bronk, M. Mulholland, D. Capone, and E. Carpenter [eds.], Nitrogen in the marine environment, 2nd ed. Academic.

Leynaert, A., P. Treguer, C. Lancelot, and M. Rodier. 2001. Silicon limitation of biogenic silica production in the Equatorial Pacific. Deep-Sea Res. I **48:** 639–660.

Martin-Jézéquel, V., M. Hildebrand, and M. A. Brzezinski. 2000. Silicon metabolism in diatoms: Implications for growth. J. Phycol. **36:** 821–840, doi:10.1046/j.1529-8817.2000.00019.x

Nelson, D. M., and M. A. Brzezinski. 1997. Diatom growth and productivity in an oligotrophic midocean gyre: A 3-yr record from the Sargasso Sea near Bermuda. Limnol. Oceanogr. **42:** 473–486, doi:10.4319/lo.1997.42.3.0473

———, ———, D. E. Sigmon, and V. M. Franck. 2001. A seasonal progression of Si limitation in the Pacific sector of the Southern Ocean. Deep-Sea Res. II **48:** 3973–3995.

———, and Q. Dortch. 1996. Silicic acid depletion and silicon limitation in the plume of the Mississippi River: Evidence from kinetic studies in spring and summer. Mar. Ecol. Prog. Ser. **136:** 163–178, doi:10.3354/meps136163

———, J. J. Goering, S. S. Kilham, and R. R. L. Guillard. 1976. Kinetics of silicic acid uptake and rates of silica dissolution in marine diatom *Thassiosira pseudonana*. J. Phycol. **12:** 246–252.

Scharek, R., M. Latasa, D. M. Karl, and R. R. Bidigare. 1999*a*. Temporal variations in diatom abundance and downward vertical flux in the oligotrophic North Pacific gyre. Deep-Sea Res. I **46:** 1051–1075.

———, L. M. Tupas, and D. M. Karl. 1999*b*. Diatom fluxes to the deep sea in the oligotrophic North Pacific gyre at Station ALOHA. Mar. Ecol. Prog. Ser. **182:** 55–67, doi:10.3354/meps182055

Shcherbina, A. Y., M. C. Gregg, M. H. Alford, and R. R. Harcourt. 2009. Characterizing thermohaline intrusions in the North Pacific Subtropical Frontal Zone. J. Phys. Oceanogr. **39:** 2735–2756, doi:10.1175/2009JPO4190.1

———, ———, ———, and ———. 2010. Three-dimensional structure and temporal evolution of submesoscale thermohaline intrusions in the North Pacific Subtropical Frontal Zone. J. Phys. Oceanogr. **40:** 1669–1689, doi:10.1175/2010JPO4373.1

Utermöhl, H. 1958. Zur Vervollkommung der quantitativen phytoplankton-methodik. Mitt. Int. Ver. Theor. Angew. Limnol. **9:** 1–38. [For the improvement of quantitative phytoplankton methodology.]

Venrick, E. L. 1974. The distribution and significance of *Richelia intracellularis* Schmidt in the North Pacific Central Gyre. Limnol. Oceanogr. **19:** 437–445, doi:10.4319/lo.1974.19.3.0437

———. 1988. The vertical distributions of chlorophyll and phytoplankton species in the North Pacific central environment. J. Plankton Res. **55:** 987–998, doi:10.1093/plankt/10.5.987

Villareal, T. A. 1990. Laboratory culture and preliminary characterization of the nitrogen-fixing *Rhizosolenia–Richelia* symbiosis. Pubbl. Staz. Zool. Napoli. I: Mar. Ecol. **11:** 117–132, doi:10.1111/j.1439-0485.1990.tb00233.x

———. 1991. Nitrogen-fixation by the cyanobacterial symbiont of the diatom genus *Hemiaulus*. Mar. Ecol. Prog. Ser. **76:** 201–204, doi:10.3354/meps076201

———, L. Adornato, C. Wilson, and C. A. Schoenbaechler. 2011. Summer blooms of diatom–diazotroph assemblages and surface chlorophyll in the North Pacific gyre: A disconnect. J. Geophys. Res.-Oceans **116:** C03001, doi:10.1029/2010JC006268

———, C. G. Brown, M. A. Brzezinski, J. W. Krause, and C. Wilson. 2012. Summer diatom blooms in the North Pacific Subtropical Gyre: 2008–2009. PLoS ONE **7:**e33109, doi:10.1371/journal.pone.0033109

Welschmeyer, N. A. 1994. Fluorometric analysis of chlorophyll *a* in the presence of chlorophyll *b* and pheopigments. Limnol. Oceanogr. **39:** 1985–1992, doi:10.4319/lo.1994.39.8.1985

White, A. E., Y. H. Spitz, and R. M. Letelier. 2007. What factors are driving summer phytoplankton blooms in the North Pacific Subtropical Gyre? J. Geophys. Res.-Oceans **112:** C12006, doi:10.1029/2007JC004129

Wilson, C. 2003. Late summer chlorophyll blooms in the oligotrophic North Pacific Subtropical Gyre. Geophys. Res. Lett **30:** 1942, doi:10.1029/2003GL017770

Associate editor: Robert R. Bidigare

Received: 29 July 2011
Accepted: 26 March 2012
Amended: 02 April 2012